J Mater Sci (2009) 44:3413–3419
DOI 10.1007/s10853-009-3453-4

In situ synthesis of transparent fluorescent ZnS–polymer nanocomposite hybrids through catalytic chain transfer polymerization technique

Li Chen · Caifeng Wang · Qing Li · Shengyang Yang · Linrui Hou · Su Chen

Received: 6 February 2009 / Accepted: 31 March 2009 / Published online: 29 April 2009

Abstract We report the controllable synthesis of zinc sulfide (ZnS) nanocrystals (NCs)/polymer transparent nanocomposite hybrids in situ based on the catalytic chain transfer polymerization (CCTP) technique. Firstly, a polymeric ligand PMAA [PMAA = poly(acrylic acid)] with controllable low-molecular-weight and a terminal double bond was synthesized through CCTP. Secondly, with the use of this versatile polymeric ligand containing a large number of anchors as the stabilizer, the ZnS NCs were fabricated. Finally, the surface polymeric ligands containing terminal double bonds were copolymerized with methyl methacrylate monomer to form NCs–polymer hybrids through free radical polymerization. The properties of as-prepared ZnS NCs and their nanocomposite hybrids were thoroughly investigated by Fourier transform Raman spectra, Fourier transform infrared spectrum, transmission electron microscope, ultraviolet–visible, photoluminescence, and thermogravimetric analyses measurements. The spectroscopic studies reveal that ZnS–polymer nanocomposite hybrids have good optical properties.

Introduction

In the past few decades, the exploration of novel composites based on semiconductor nanocrystals (NCs) has attracted extensive scientific and industrial interests as a consequence of their strong size-dependent properties, unique optical, and electronic features [1–6]. To be specific, zinc sulfide (ZnS) NC is the most typical and important semiconductor material with wide bandgap (~3.6 eV in bulk) and has exhibited great potential applications in wide areas, including light-emitting devices, photonic crystals, nonlinear optical devices, and biological labels [7–15]. Unfortunately, it still remains a challenge to stabilize NCs into bulk polymer matrices so as to overcome the quenching of photoluminescence (PL) resulting from phase separation and NC aggregation [16, 17]. For this purpose, the surface chemistry of the NCs is of major importance, because functional surface ligands can serve as linkers between the particles and polymer matrices [18–25].

In principle, a functional ligand consists of an anchor group, an outer functionality, and a spacer between them [26]. Up to now, much effort has been devoted to the surface modification of NCs for improving their inherent stability and the luminescence intensity [27–30]. For example, possible organic anchor groups for semiconductors are provided by amines, oxides, and thiols, which have different affinities to the NC surface and alter the fluorescence properties to a different degree. However, a major problem in linker chemistry is that the stability of the complex relies on the strength of only one chemical bond. If either the anchor to the NC surface or the functional docking bond breaks, the whole complex would dissociate [31–36]. Therefore, the incorporation of fluorescent NCs with various functional polymer ligands containing many anchor points, such as diblock ionomers [37], homopolymers [38, 39], block copolymers [40, 41], polymer micelles [42–44], or dendronized polymers [45], would be extremely useful to improve the interaction between the polymer ligands and NCs. Still, it is essential that the polymer ligands can form strong chemical bonds with polymers as

L. Chen · C. Wang · Q. Li · S. Yang · L. Hou · S. Chen (✉)
State Key Laboratory of Material-Oriented Chemical Engineering, College of Chemistry and Chemical Engineering, Nanjing University of Technology, No. 5 Xin Mofan Rd., Nanjing 210009, People's Republic of China
e-mail: chensu@njut.edu.cn; prcscn@yahoo.com.cn

to improve the compatibility between NCs and polymer matrices. For these purposes we are focused on addressing this problem by introducing a new versatile polymer ligand prepared by catalytic chain transfer polymerization (CCTP) technique, where the interaction between the polymer ligands and NCs is increased by the presence of multiple anchor groups and outer double bond functionality. As reported in literatures, CCTP is a powerful synthetic route to produce a relative low-molecular-weight polymer chain with a terminal double bond [46, 47].

In this study, we take the advantage of this characteristic of CCTP to design a multianchor polymer ligand based on poly(acrylic acid), which contain carboxyl groups' multiple anchors coordinated with NCs and terminal double bond tethered to the polymer matrices. Scheme 1 presents the overall preparative strategy for producing ZnS/PMAA/PMMA nanocomposite hybrids. Firstly, PMAA macromonomers bearing multifunctional groups (–COOH) and unsaturated end vinyl groups were fabricated through CCTP with the presence of chain transfer agent CoBF (bis(aqua)bis((difluoroboryl)dimethylglyoximato)cobalt(II)). Subsequently, ZnS NCs were prepared by using the as-synthesized PMAA-functionalized ligand under room temperature. Finally, the PMAA-functionalized ZnS NCs containing terminal double bonds were copolymerized with methyl methacrylate (MMA) monomers to prepare ZnS/PMAA/PMMA nanocomposite hybrids through free radical polymerization. Typically, NCs incline to aggregate in the polymer matrix as a result of their high surface area and surface energy. Herein, however, the predesigned polymer ligand can effectively connect NCs to polymers as a bridge to prevent the aggregation and result in the formation of well-stabilized transparent ZnS–polymer nanocomposite hybrids, therein obtaining well-stabilized and highly enhanced luminescent NCs–polymer hybrids in this case.

Experimental

Materials

Methacrylic acid (MAA) (Aldrich, 99%) and MMA (Aldrich, 99%) were purified by distillation under reduced pressure and stored at −5 °C. The initiators, 2,2′-azoisobutyronitrile (AIBN) and 2,2-Azobis(2-(2-imidazolin-2-yl)propane)dihydrochloride (VA-044) were purified by repeated recrystallization from methanol. Zinc chloride ($ZnCl_2$), sodium sulfide ($Na_2S \cdot 9H_2O$), and *N*,*N*-dimethylformamide (DMF), 2-propanol, were purchased from Aldrich and used without further purification. The cobalt catalyst CoBF was prepared according to a procedure reported by Bakac and Espenson [48]. CoBF was analyzed using elemental analysis (Calcd.: C 22.80%, H 3.83%, N 13.30%; Found: C 22.86%, H 3.89%, N 13.40%). The structure of CoBF is shown in Scheme 2.

Synthesis of PMAA macromonomers

In a typical reaction, 0.3 g of azo initiator VA-044 and 13 mg of CoBF dissolved in 2 mL acetone were added to DI water (150 mL). The mixture was heated under nitrogen atmospheres at 55 °C after degassing using six alternating cycles of evacuation and pressurization with high purity nitrogen (starting with evacuation). Polymerization carried out after the injection of a CoBF/MAA mixture (7.5 mg CoBF dissolved in 74.0 g MAA). The reaction was allowed to proceed for 2 h with continuous stirring under nitrogen atmosphere and then quenched with an ice-water bath. The as-prepared PMAA was precipitated in diethyl ether, and then redissolved in DI water and reprecipitated in diethyl ether for several times. The product was subsequently

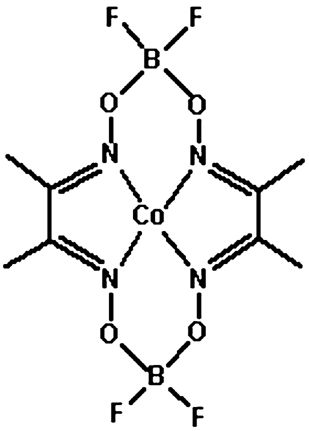

Scheme 2 Structure of cobalt catalyst CoBF

Scheme 1 A schematic illustration of the synthesis process of ZnS/PMAA/PMMA nanocomposite hybrids

separated by centrifugation, and dried under vacuum for various characterizations and post-synthesis.

Synthesis of ZnS NCs and ZnS/PMAA/PMMA nanocomposite hybrids

A DMF (4 mL) solution of 1.25 mmol $ZnCl_2$ was added dropwise into a DMF (40 mL) solution of PMAA macromonomer (12.5 mmol carboxyl groups) under continuously stirring. And then, 0.9 mmol of $Na_2S \cdot 9H_2O$ (in 4 mL DI water) was dropped to the above complex mixture and was keep on stirring for 2 h at room temperature. ZnS/PMAA/PMMA nanocomposite hybrids were synthesized using ZnS/PMAA and MMA monomer as raw materials by free radical polymerization. A solution of AIBN and MMA was added dropwise to a proper amount of as-prepared ZnS NCs suspension with vigorously stirring under nitrogen atmosphere at 70 °C for 4.5 h (AIBN: MMA = 0.003: 1 w/w, PMAA: MMA = 1: 5 w/w, MMA monomers accounts for 10 wt% of the total solution). More clear synthesis procedure is shown in Scheme 1.

Characterization

Molecular weight distributions were analyzed by gel permeation chromatography (GPC) using a Waters 1515 isocratic pump, a Waters 717 plus autosampler, a column set consisting of three Waters Styragel columns (7.8 × 300 mm^2) HR4, HR3, HR1, and a Waters 2414 differential refractive index detector. Tetrahydrofuran (TEDIA, HPLC grade) was used as eluent at 0.6 mL/min. Calibration of the GPC equipment was carried out with narrow polystyrene standards (molecular weight range 1,200–538,000 g/mol). ^{1}H-NMR spectra were acquired with a BRUKER DAX 500 with TMS as internal standard in deuterate DMF. Fourier transform Raman (FT-Raman) spectroscopy were performed on an NXR FT-Raman Module by sharing interferometer installed in the Fourier transform infrared (FT-IR) bench. The Raman optics system is comprised of Nd:YVO4 laser operating at 1064 nm, sample holders, an InGaAs detector, and a CaF_2 beam splitter. Spectra of fine powder samples pressed in a suitable sample holder were then collected with a laser power of 1.0 W, a mirror velocity of 0.3165 cm/s, and 128 scans at a resolution of 8 cm^{-1}. A high-resolution transmission electron microscope (HRTEM) was conducted on JEOL-2010 TEM at an acceleration of 200 kV and used to observe the morphology of the nanocomposites. The samples were dispersed in DMF, and a drop of the solution was placed on a copper grid that was left to dry before transferring into the TEM sample chamber. Ultraviolet–visible (UV–Vis) absorption spectra were taken with a Perkin-Elmer Lambda 900 UV–Vis spectrometer with the scan range 260–450 nm using DMF as solvent. PL spectra were measured on a Cary Eclipse fluorescence spectrophotometer photoluminescence spectrophotometer at room temperature operating with a 300 nm laser beam as a light source with Xe-lamp as excited source, tube voltage was 600 V, the excitation and emission slits were 5 nm. FT-IR spectra were recorded on a NICOLET-NEXUS670 spectrometer. The samples were grounded with KBr crystal and the mixture of them was pressed into a flake for IR measurement. The sample was prepared by drying in a vacuum oven at 90 °C for 2 days at a reduced pressure for solvent removal. Thermogravimetric analysis (TGA) measurement was performed for testing the heat loss of ZnS/PMAA/PMMA hybrids using a thermogravimetric apparatus Shimadzu-TGA 50 under nitrogen atmosphere. Analysis was carried out with a heating rate of 10 °C/min from 38 to 600 °C.

Results and discussion

The development of NCs–polymer hybrid materials faces several challenges in terms of chemical compatibility and retaining NCs optical properties. Most reported study with in situ polymerization focused on a ligand-exchange step prior to polymerization in order to protect the NCs from PL intensity loss. In this study, we report the synthesis of NCs–polymer with CCTP technique. CCTP is a powerful synthetic route to produce a relative low-molecular-weight dead polymer chain with a terminal double bond [49]. Here, we follow this characteristic of CCTP to design the polymer ligand: the PMAA macromonomer with a terminal double bond was prefabricated as a multianchor polymeric ligand $\left(\overline{M}_n = 2848\ \text{g/mol},\ \text{PDI} = 1.08\right)$ through CCTP at first. Subsequently, ZnS NCs were prepared under room temperature with the aid of the presynthesized functionalized ligand as the stabilizer. Finally, the surface polymeric ligands containing terminal double bonds were subsequently polymerized with MMA monomer to form NCs–polymer hybrids through free radical polymerization, therein obtaining well-stabilized and highly enhanced luminescent NCs–polymer hybrids in this case.

The evidence for the successfully preparation of PMAA macromonomer with unsaturated end vinyl groups through CCTP can be demonstrated by NMR measurement. As seen in Fig. 1, vinyl groups in the end of PMAA macromonomer are determined by ^{1}H-NMR spectroscopy from the region at 5.5–6.5 ppm. In the expanded inset, “p” shows the expected vinylic ω-end group in PMAA macromonomer, and “m” indicates trace monomer in the final product isolated by evaporation of water. It would be worthy to indicate that it is very difficult and even impossible to remove all residual MAA monomer in the product. And thus the weak peaks “m” would still exist.

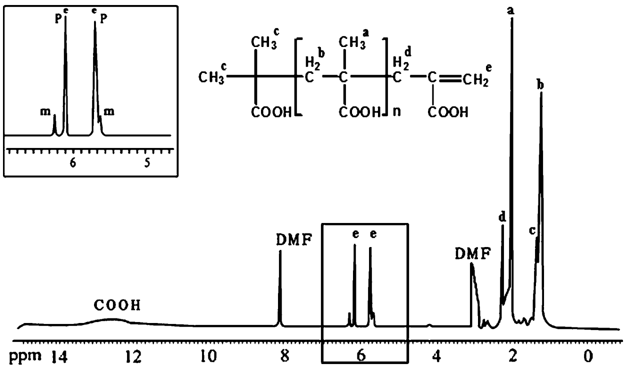

Fig. 1 ^{1}H-NMR (300 MHz, DMF) spectrum of PMAA macromonomer prepared by using CCTP in DMF (*p* vinyl protons in the product, *m* vinyl protons in the monomer)

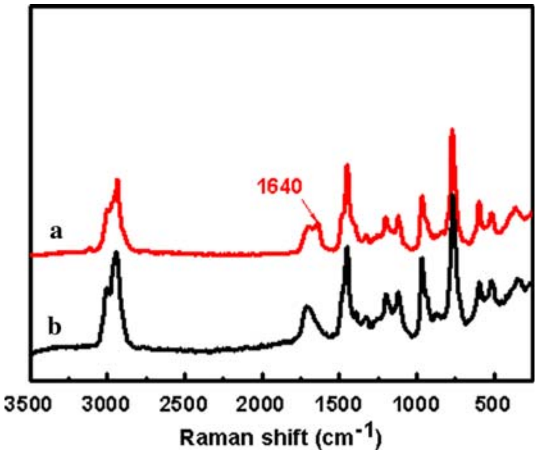

Fig. 2 Raman shift spectra of (a) PMAA prepared through free radical polymerization, (b) PMAA macromonomer prepared by using CCTP

Analogue result is also obtained in the literature [50]. Moreover, the chemical structures of the PMAA macromonomer prepared via CCTP can be characterized by Raman spectra. Figure 2 is Raman spectra of PMAA macromonomer prepared by using CCTP and corresponding PMAA prepared by free radical polymerization for comparison (Fig. 2a). As seen in Fig. 2, the Raman shift appeared at 1640 cm^{-1} in Fig. 2b can be assigned to the unsaturated carbon–carbon double bonds in end-groups of the PMAA macromonomer, which is consistent with the result of ^{1}H-NMR. These results also present that we have successfully synthesize the PMAA macromonomer with terminal unsaturated double bonds by using CCTP technique.

Figure 3 displays HRTEM images with low-magnification and high-magnification of PMAA-capped ZnS NCs by using as-synthesized PMAA macromonomer as the ligand. As seen in Fig. 3a, we can directly observe a uniform size distribution of ZnS NCs in homogeneous oligomers medium without any aggregation, owing to the introduction of PMAA multianchor sites improving the interaction between ZnS NCs and PMAA ligands. By scrutiny of ZnS NCs shown in Fig. 3a, the ZnS NCs were found to have a narrow size distribution with average size of about 2.5–3.0 nm. A typical high-magnification HRTEM image is presented in Fig. 3b, the appearance of distinct lattice planes on the magnified ZnS NCs image confirms production of the high-quality crystalline ZnS nanoparticles. Detailed analysis on the lattice fringes gives an interplanar distance of about 0.31 nm, which agrees well with the lattice spacing of the (111) planes of cubic ZnS ($d_{111} = 0.312$ nm for cubic ZnS) [11]. The above results also present that as-prepared ZnS NCs with PMAA oligomer as the polymeric ligand still exhibit as quantum dots. The dispersibility and stabilization of ZnS NCs could be enhanced when ZnS NCs are embedded in the PMAA chains.

ZnS/PMAA/PMMA nanocomposite hybrids were synthesized by copolymerization of PMAA-functionalized ZnS NCs and MMA monomers using AIBN as the initiator. The FT-IR spectrum of ZnS/PMAA/PMMA nanocomposite is shown in Fig. 4. Strong absorption peak noticed at 1160 cm^{-1} shows that abundant C–O groups are tethered on the surface of ZnS NCs. The stretching frequencies of the C=O bonds located at 1720 cm^{-1}, C–O bonds at 1400 cm^{-1} and 1549 cm^{-1}, and O–H at 2920–3000 cm^{-1}, respectively, are attributed to carboxylate groups. It further confirms that the ZnS/PMAA/PMMA nanocomposite hybrids have been successfully prepared.

In order to investigate the optical properties of the NCs and the nanocomposite hybrids, the pure PMMA, ZnS NCs using PMAA macromonomer as the ligand, and ZnS/PMAA/PMMA nanocomposite hybrids were characterized by UV–Vis absorption and PL spectra, respectively. As seen in Fig. 5, the pure PMAA shows a weak absorption peak at a wavelength of 265 nm, whereas ZnS NCs stabilized with PMAA macromonomer and ZnS/PMAA/PMMA nanocomposite hybrids show the intense characteristic UV absorption peak at about 272 nm (4.56 eV). Compared with the UV absorption peak of bulk ZnS which is noticed at about 338 nm (3.71 eV), the absorption peak of ZnS NCs and NCs–polymer nanocomposite hybrids is greatly blue-shifted because of a quantum size effect caused by the confinement of the electron and hole in a small cubage. The calculated particle size of as-prepared functional ZnS NCs according to Brus [51, 52] formula is about 2.6 nm, which is in good agreement with the result of TEM measurement. Another indication from Fig. 5 that the position of UV absorption peak of ZnS/PMAA/PMMA nanocomposite hybrid does not alter indicates that the particle size of ZnS

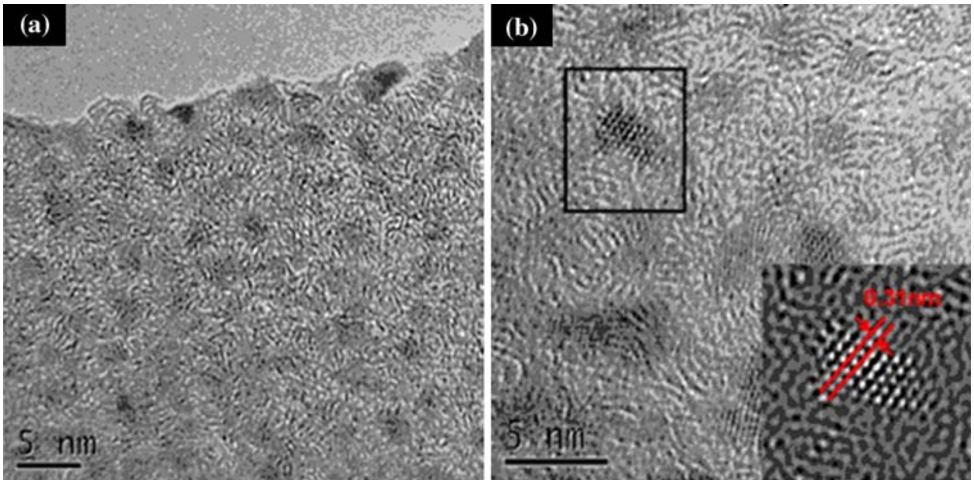

Fig. 3 **a** Low-magnification and **b** high-magnification HRTEM images of PMAA-capped ZnS NCs

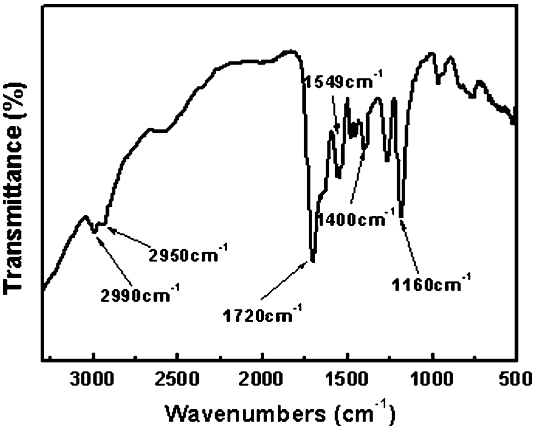

Fig. 4 FT-IR spectrum of ZnS/PMAA/PMMA nanocomposite hybrid ($COOH^-/Zn^{2+}/S^{2-} = 10/1/0.6$ mol/mol, MMA/PMAA = 5:1 w/w, AIBN/MMA = 0.3 wt%, reaction time: 4.5 h)

NCs in this nanocomposite hybrid after copolymerization between ZnS NCs and PMMA matrix does not change.

As a typical semiconductor, ZnS NCs display interesting optical properties. With the ZnS NCs embedded in the PMMA matrix, ZnS/PMAA/PMMA nanocomposite hybrids also show excellent optical characteristic property. Figure 6 demonstrates the PL emission spectra of pure PMAA, ZnS NCs stabilized with PMAA macromonomer, and ZnS/PMAA/PMMA nanocomposite hybrids with excitation at 300 nm. ZnS NCs and ZnS/PMAA/PMMA nanocomposite hybrids show the characteristic emission peak of ZnS NCs at 414 nm, which is attributed to recombination from the excitonic state in the crystallite interior. Moreover, an increase in PL intensity was observed after the functionalized ZnS NCs were embedded in the PMMA matrix, which can be ascribed to the local field enhancement effect

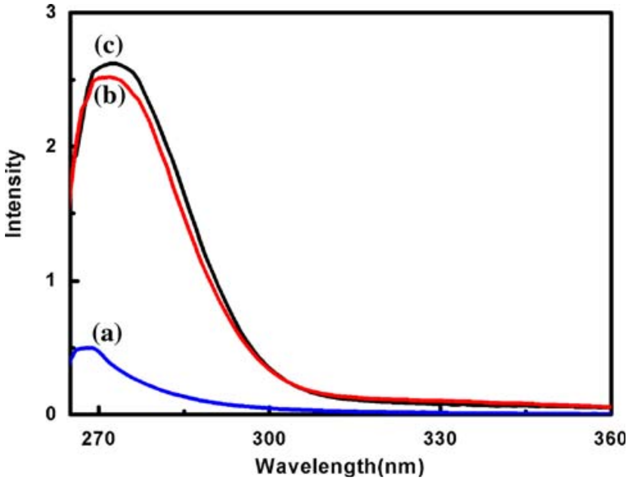

Fig. 5 UV–Vis absorption spectra of (a) pure PMAA, (b) ZnS NCs stabilized with PMAA macromonomers ($COOH^-/Zn^{2+}/S^{2-} = 10/1/0.6$ mol/mol; solvent:H_2O/DMF = 2:10 w/w; reaction time: 2 h), and (c) ZnS/PMAA/PMMA nanocomposite hybrid (MMA/PMAA = 5:1 w/w, AIBN/MMA = 0.3 wt%, reaction time: 4.5 h, dispersed in DMF)

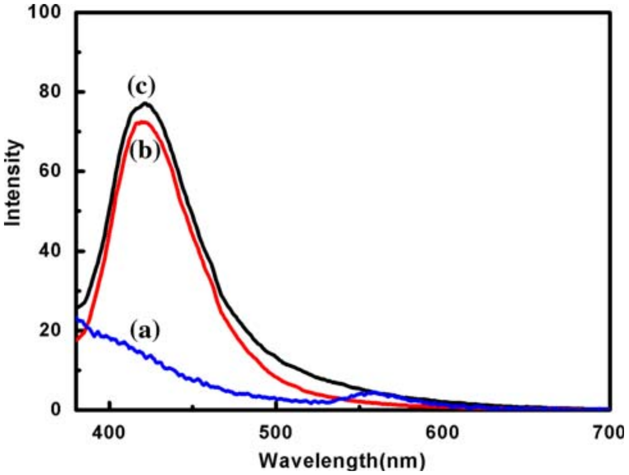

Fig. 6 The PL emission spectra of (a) pure PMAA, (b) ZnS NCs stabilized with PMAA macromonomer ($COOH^-/Zn^{2+}/S^{2-} = 10/1/0.6$ mol/mol; solvent:H_2O/DMF = 2:10 w/w; reaction time: 2 h), and (c) ZnS/PMAA/PMMA nanocomposite hybrid (MMA/PMAA = 5:1 w/w, AIBN/MMA = 0.3 wt%, reaction time: 4.5 h, dispersed in DMF)

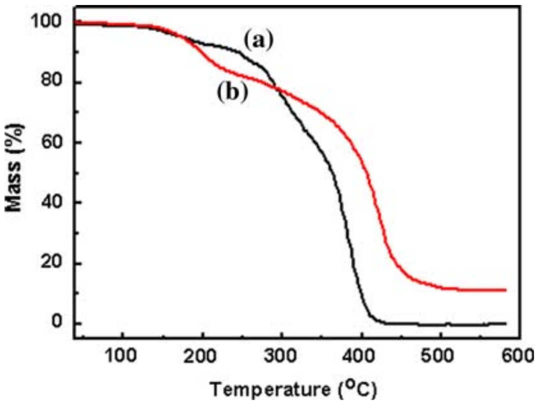

Fig. 7 TGA curves of (a) pure PMMA polymer (AIBN/MMA = 0.3 wt%, reaction time: 4.5 h); and (b) ZnS/PMAA/PMMA nanocomposite hybrid (MMA/PMAA = 5:1 w/w, AIBN/MMA = 0.3 w%, reaction time: 4.5 h)

[53]. These ZnS NC cores are well surrounded by dielectric polymer ligands, which have much lower refractive indices than the inorganic semiconductors, and hence bear a larger enhancement factor. Also, this polymeric ligand can greatly improve the compatibility between ZnS NCs and polymer matrix, overcoming the fluorescence quenching resulting from phase separation [54].

The thermal stability of the products was investigated with TGA. Figure 7 shows TGA curves of pure PMMA and ZnS/PMAA/PMMA nanocomposite hybrids, respectively. The initial degradation temperature starts from 140 °C, which is attributed to the presence of DMF in the samples. The improvement in thermal stability for ZnS/PMAA/PMMA nanocomposite hybrid after incorporating ZnS NCs by in situ copolymerization was observed. By comparison, ZnS/PMAA/PMMA nanocomposite hybrid shows higher thermal stability in the temperature range of the degradation step (between 300 and 450 °C at a heating rate of 10 °C/min) than that of pure PMMA prepared by free radical polymerization, which might be attributed to that the interfacial interactions between the PMMA and ZnS NCs can be greatly enhanced by using ZnS NCs in situ growth in PMMA matrix.

Conclusions

In summary, we have firstly reported the synthesis of functionalized ZnS NCs and the transparent ZnS/PMAA/PMMA nanocomposite by using CCTP technique. In this in situ polymerization procedure, polymeric oligomer ligands were designed to act not only as stabilizer, but also as anchor sites in the composites. In addition, we have found that the dispersibility and processability of ZnS NCs are significantly improved by grafting polymers onto their surfaces. The spectroscopic studies indicate that as-prepared ZnS–polymer hybrids exhibit good PL stability without polymerization-induced fluorescence quenching. These findings reveal that controllable polymerization methods, for example CCTP, can provide an ideal process for synthesis of stable NCs–polymer nanocomposite hybrids.

Acknowledgement This study was supported by Natural Science Foundations (NSFs) of China (Grant No. 20576053, 20606016), NSF (NASA) of China (Grant No. 10676013), and the NSF of the Jiangsu Higher Education Institutions of China (Grant No. 07KJA53009).

References

1. Steigerwald ML, Brus LE (1990) Acc Chem Res 23:183
2. Alivisatos AP (1996) J Phys Chem 100:13226
3. Loss D, DiVincenzo DP (1998) Phys Rev A 57:120
4. Murray CB, Kagan CR, Bawendi MG (2000) Annu Rev Mater Sci 30:545
5. Burda C, Chen X, Narayanan R et al (2005) Chem Rev 105:1025
6. Cao XD, Li CM, Bao QL et al (2007) Chem Mater 19:3733
7. Hwang JI, Oh M, Kim L et al (2005) Curr Appl Phys 5:31
8. Bai C, Fang Y, Zhang Y et al (2004) Langmuir 20:263
9. Pich A, Hain J, Lu Y et al (2005) Macromolecules 38:6610
10. Ni Y, Ge X, Zhang Z (2005) Mater Sci Eng 119:51
11. Guo L, Chen S, Chen L (2007) Colloid Polym Sci 285:1593
12. Lü C, Cui Z, Wang Y et al (2003) J Mater Chem 13:2189
13. Lü C, Cheng Y, Liu Y et al (2006) Adv Mater 18:1188
14. Hirai T, Watanabe T, Komasawa I (2000) J Phys Chem B 104:8962
15. Chen S, Zhu J, Shen Y et al (2007) Langmuir 23:850
16. Murray CB, Norris DJ, Bawendi MG (1993) J Am Chem Soc 115:8706
17. Lee J, Sundar VC, Heine JR et al (2000) Adv Mater 12:1102
18. Lopes WA, Jaeger HM (2001) Nature 414:735
19. Böker A, Lin Y, Chiallerini K et al (2004) Nat Mater 3:302
20. Lin Y, Böker A, He J et al (2005) Nature 434:55
21. Mackay ME, Tuteja A, Duxbury PM et al (2006) Science 311:1740
22. Balazs AC, Emrick T, Russell TP (2006) Science 314:1107
23. Wang X, Guerin G, Wang H et al (2007) Science 317:644
24. Chen S, Sui JJ, Chen L et al (2005) J Polym Sci Part A Polym Chem 43:1670
25. Chen S, Sui JJ, Chen L (2004) Colloid Polym Sci 283:66
26. Potapova I, Mruk R, Hubner C et al (2005) Angew Chem Int Ed 44:2437
27. Wang CW, Moffitt MG (2004) Langmuir 20:11784
28. Guo W, Li JJ, Wang YA et al (2003) J Am Chem Soc 125:3901
29. Chen KB, Chen MH, Yang SH et al (2006) J Polym Sci Polym Chem 44:5378
30. Chen L, Zhu J, Li Q et al (2007) Eur Polym J 43:4593
31. Potapova I, Mruk R, Prehl S et al (2003) J Am Chem Soc 125:320
32. Watson KJ, Zhu J, Nguyen ST et al (1999) J Am Chem Soc 121:462
33. Skaff H, Ilker MF, Coughlin EB et al (2002) J Am Chem Soc 124:5729
34. Zhang H, Wang C, Li M et al (2005) Chem Mater 17:4783
35. Korth BD, Keng P, Shim I et al (2006) J Am Chem Soc 128:6562
36. Choudhury KR, Sahoo Y, Prasad PN (2005) Adv Mater 17:2877
37. Moffitt M, McMahon L, Pessel V (1995) Chem Mater 7:1185
38. Mayer ABR, Mark JE (1998) Eur Polym J 34:103

39. Roan JR (2001) Phys Rev Lett 86:1027
40. Qi L, Colfen H, Antonietti M (2001) Nano Lett 1:61
41. Yu K, Wang H, Han Y (2007) Langmuir 23:8957
42. Moffitt M, Vali H, Eisenberg A (1998) Chem Mater 10:1021
43. Zhao HY, Douglas EP, Harrison BS et al (2001) Langmuir 17:8428
44. Zhao HY, Douglas EP (2002) Chem Mater 14:1418
45. Zhang Y, Chen Y, Niu H et al (2006) Small 2:1314
46. Gridnev AA, Ittel SD (2001) Chem Rev 101:3611
47. Heuts JPA, Roberts GE, Biasutti JD (2002) Aust J Chem 55:381
48. Bakac A, Espenson JH (1984) J Am Chem Soc 106:5197
49. Suddaby KG, Sanayei RA, Rudin A et al (1991) J Appl Polym Sci 43:1565
50. Haddleton DM, Depaquis E, Kelly E et al (2001) J Polym Sci Polym Chem 39:2378
51. Brus LE (1984) J Chem Phys 80:4403
52. Brus LE (1986) J Phys Chem 90:2555
53. Wang Y, Herron N (1991) J Phys Chem 95:525
54. Paquet C, Kumacheva E (2007) Adv Funct Mater 17:3105